

## Chapter 4. Application to the optical switch

### 4-1. Introduction

Many applications for devices of GaAs on Si have been studied, but still now, due to the biaxial tensile stress and to high density of misfit dislocations, limited applications have been found in making active devices where much power is needed. However, applications to passive devices such as optical switches or optical modulators are not hindered by such a difficulty. In the present, it is still impossible to make integrations of all optoelectronic components on one chip on Si (including the light source, modulators and optical detectors). But considering the hybrid OEIC's (which do not have active devices), it may be possible to make them for practical uses (if the other optical components works as expected.). We need to be sure whether other optical (passive) devices can work or not on Si substrate. One interesting component fabricated in GaAs on Si is an optical switch that utilizes the quantum confined Stark-effect (QCSE).

There are many reports about the optical waveguide switch utilizing QCSE fabricated on GaAs substrate<sup>1)~5)</sup>. The characteristics of such a kind of switch are as follows:

- 1). They have the same structures as QW-laser diode and are therefore suitable for monolithic integration with a laser diode<sup>3) 4)</sup>.
- 2). High speed can be expected, because the absorption

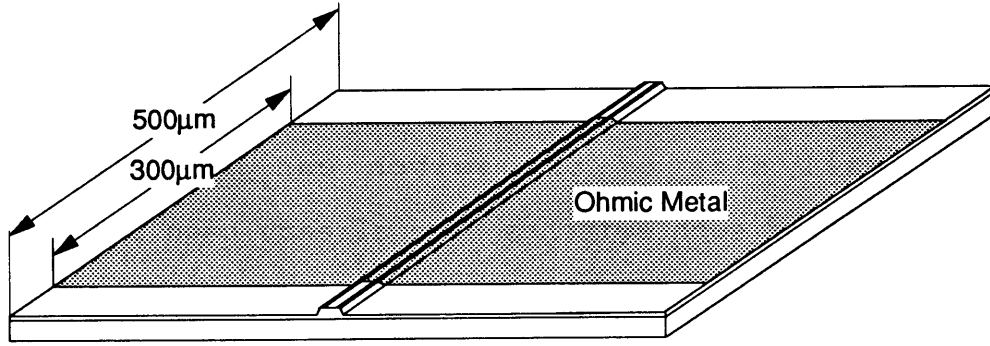
occurs by the shift of the absorption level. More than 10GHz operation device was reported<sup>5)</sup>.

3). A small size of the switch can be achieved and integrations of such switches have already been reported.

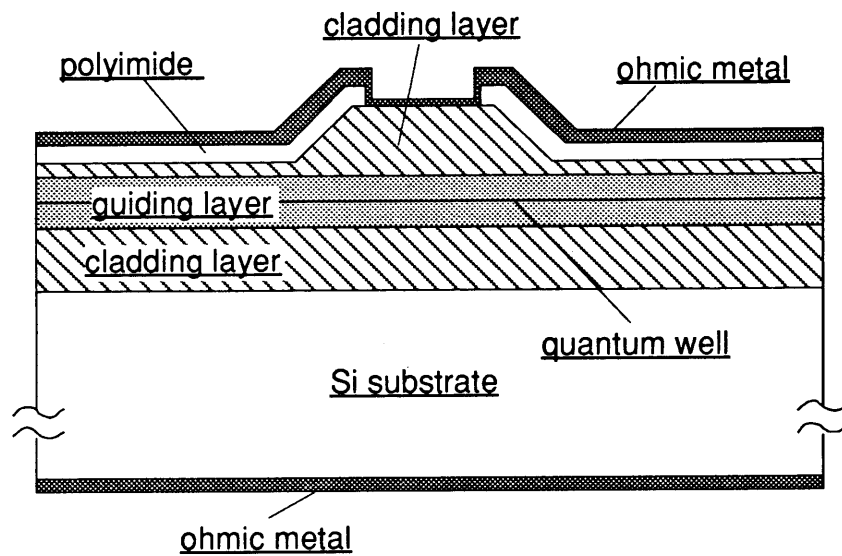
#### 4-2. Sample preparation

##### 4-2-1. Structure of the sample

The QCSE in the GaAs/AlGaAs epi-layer on Si substrate is estimated in chapter 3-4. These results indicates that it is possible to make optical switches utilizing the QCSE. We prepared a ridge type 3-dimensional optical switch shown in Fig.4-1. The 2.0 $\mu$ m width and 0.9 $\mu$ m height ridge was fabricated by wet chemical etching. The structure in the growth direction of the sample is composed of the three layers (ie. p-Al<sub>0.3</sub>Ga<sub>0.7</sub>As/Al<sub>0.25</sub>Ga<sub>0.75</sub>As/n-Al<sub>0.3</sub>Ga<sub>0.7</sub>As) on n-Si substrate. The thickness and the carrier density was the same as introduced in chapter 3-3-3. In this structure, light traveling in the guiding layer is confined to a fundamental mode at the wavelength  $\lambda < 900$ nm in both parallel and vertical directions. The crosssectional SEM image of the sample is shown in Fig.4-2. Polyimide is used for the insulator and also formed the windows for the electrode. As ohmic-metals, Au with Zn (Zn contents are 10 weight %) alloy for p-type GaAs and Au with Sb (Sb contents are 1 weight %) alloy for n-type Si are used. The sample were cleaved at 500 $\mu$ m length. The incident light of Ti:sapphire laser was



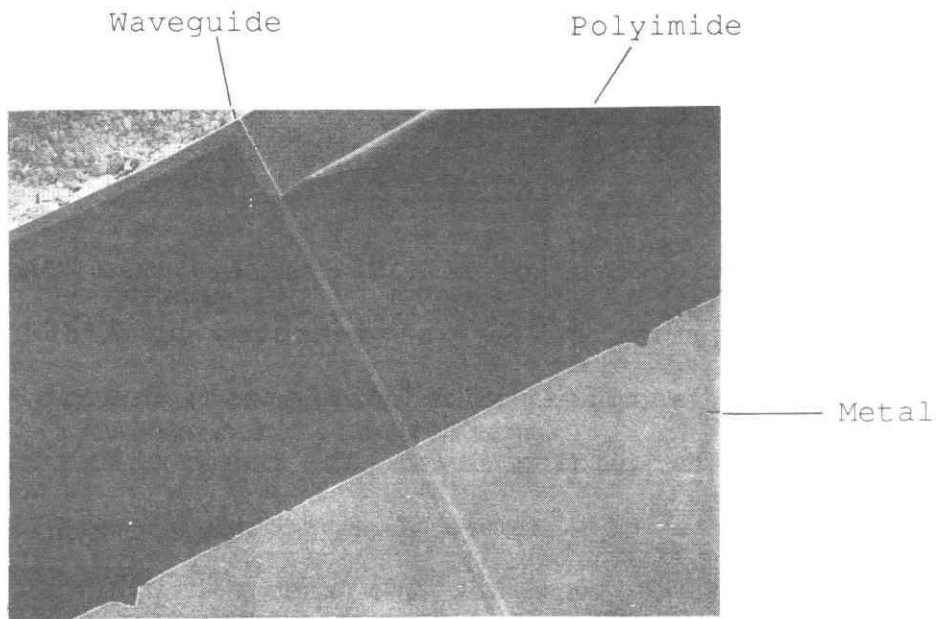
a). Sidelong view



b). Crosssectional view

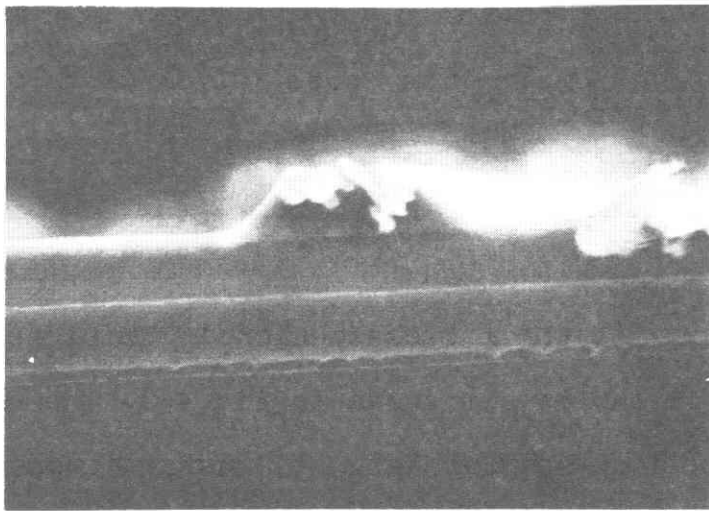
**Fig.4-1. Schematic diagram of the GaAs on Si waveguide switch using QCSE.**

The upper cladding layer was doped with Zn to  $n=1 \times 10^{18} \text{ cm}^{-3}$  and the lower with Se to  $p=1 \times 10^{18} \text{ cm}^{-3}$ . The guiding layer is undoped. Therefore p-i-n junction was formed in the waveguide.



33.3 $\mu$ m

a).Top view



1.0mm

b).Crosssectional view

Fig.4-2. The SEM pictures of the optical switch.

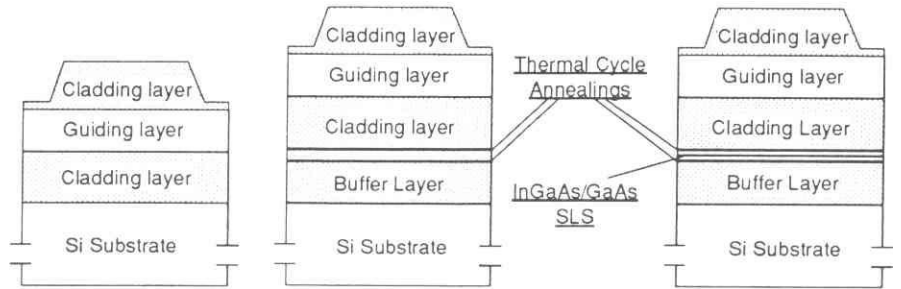
led into the cleaved facet of the sample. And the output light intensity was measured by Si detector.

#### 4-2-2. Propagation loss

The propagation loss of  $\text{Al}_{0.3}\text{Ga}_{0.7}\text{As}/\text{Al}_{0.25}\text{Ga}_{0.75}\text{As}/\text{Al}_{0.3}\text{Ga}_{0.7}\text{As}$  DH waveguides on Si was measured at  $\lambda=860\text{nm}$ . We prepared three samples with different densities of dislocations in the guiding layer. The basic structures for the guiding were the same. The samples were simple waveguides and there were not QWs and p-i-n junctions in them. The investigation of the propagation loss of the waveguide in the structure above was very important because their fundamental structures to confine the traveling light were the same as those of the optical switch prepared in 4-2-1. We could estimate the loss depending on the dislocations densities in the switch. The measured wavelength ( $\lambda=860\text{nm}$ ) is the estimated value for switching of the prepared sample at 4-2-1 ( $L_z=8.3\text{nm}$ ).

The schematics and their crosssectional TEM pictures of the prepared three samples are shown in Fig.4-3. The density of the dislocations in samples (a), (b) and (c) were about  $1 \times 10^7$ ,  $2 \times 10^6$  and  $1 \times 10^6$ , respectively. The losses were evaluated by the cut-off method. Fig.4-4 shows the results of the obtained output intensity versus sample length. The losses of the sample were 42.5dB/cm, 45.5dB/cm and 45.9dB/cm, respectively. These value are pretty large, but the actual length of the optical switch is very short. The 0.5mm

Schematics of the samples

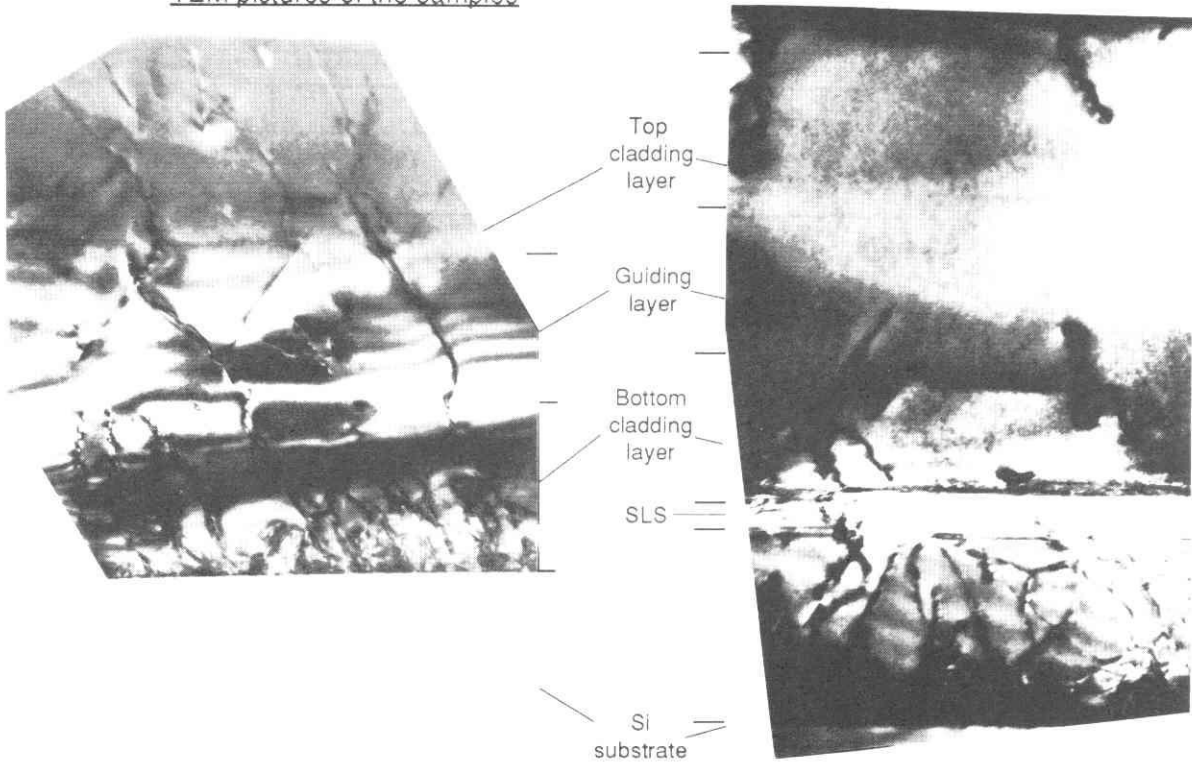


(a). Without thermal cycle annealings

(b). Two thermal cycle annealings

(c) Two thermal cycle annealings and five times SLS

TEM pictures of the samples



(a)

1.0µm

(c)

**Fig.4-3. The schematics of the sample to measure the absorption loss and their crosssectional TEM image.**

In sample (a), there are many dislocations in the guiding layer, but in (b), there are very few.

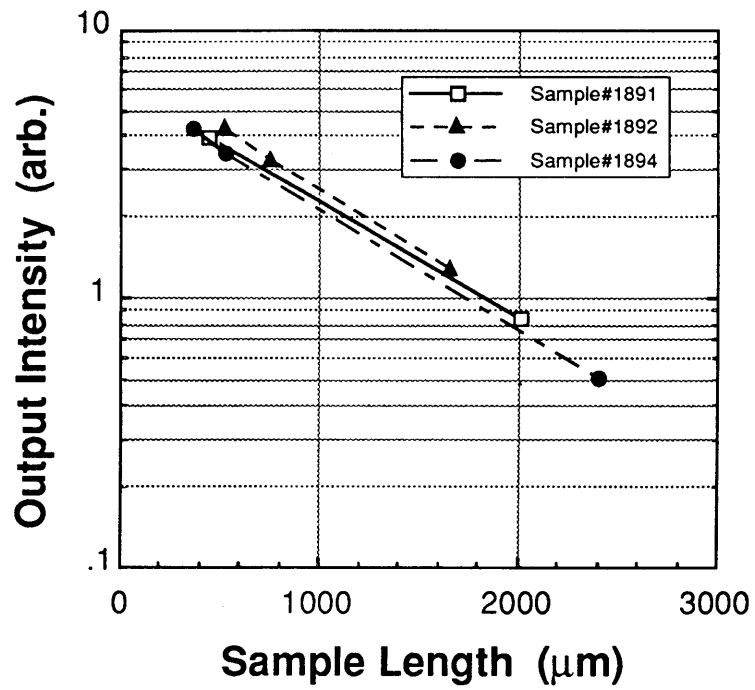


Fig.4-4. Obtained output intensity of every sample in different sample lengths.

The measured values were almost the same.

long optical switch showed more than 10dB/mm modulation (which is described in session 4-3.). With this length, the propagation loss was smaller than 3dB. The loss in every sample was almost the same. These results show that the dislocation does not effect the propagation loss so much.

#### 4-3.Properties of the switch

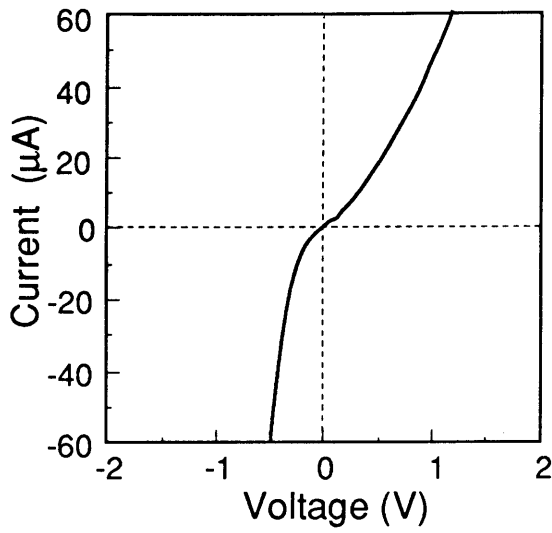
##### 4-3-1.I-V properties of the switch

The I-V characteristics of the sample were measured. Fig.4-5 shows the results measured in different regions. The basic structure of the epi-layer was the same introduced in session 4-2-1. As ohmic metals, Au on Au+Zn alloy for p-GaAs and Au on Au+Sb alloy for n-Si were used. Alloys were fabricated by the evaporation and the Au by Electric-beam-Gun. The thickness of the metal was about 0.1 $\mu$ m. A p-i-n junction in the epi-layer, and a heterojunction between Si and Al<sub>0.3</sub>Ga<sub>0.7</sub>As were fabricated in the sample. The I-V characteristics between Si and bottom n-Al<sub>0.3</sub>Ga<sub>0.7</sub>As, between p-Al<sub>0.3</sub>Ga<sub>0.7</sub>As and n-Al<sub>0.3</sub>Ga<sub>0.7</sub>As double heterojunction and between Si substrate and top p-Al<sub>0.3</sub>Ga<sub>0.7</sub>As (through the sample) are shown in Fig.4-5, a), b) and c), respectively. The properties of these are shown below:

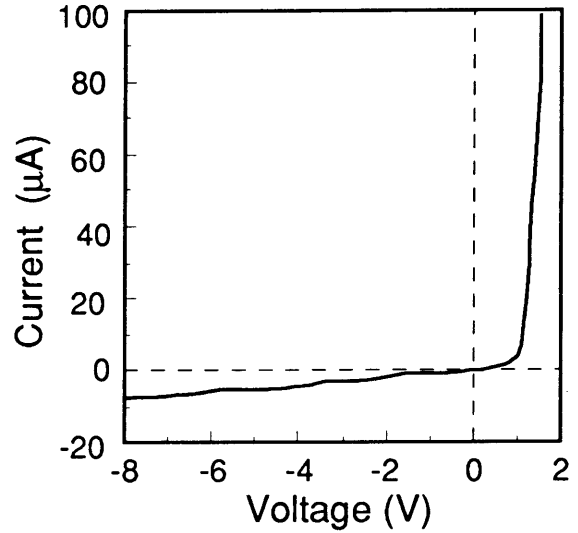
a).Between Si substrate and bottom cladding layer:

Very low resistivity is observed. Heterojunction property is not observed clearly.

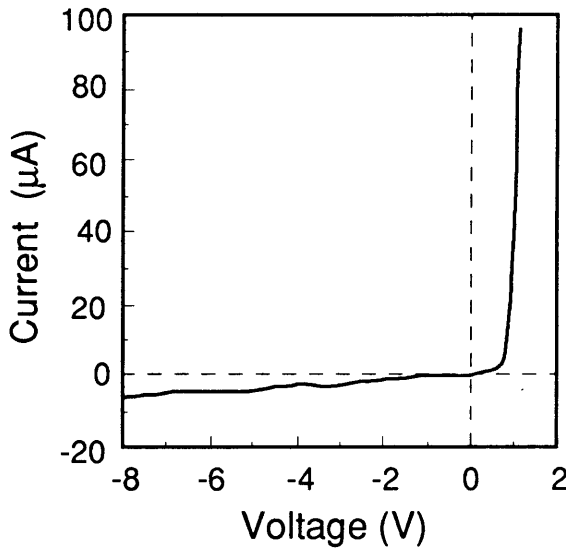
b).Between top cladding layer and bottom cladding layer:



a). I-V characteristics of B-C



b). I-V characteristics of A-B



c). I-V characteristics of A-C

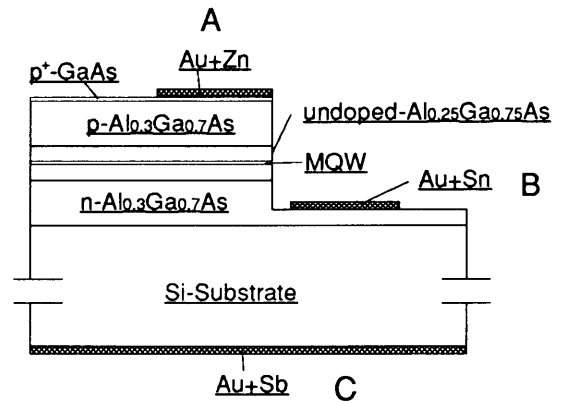


Fig.4-5. I-V characteristics of the sample.

A p-n junction property is clearly observed.

c). Between top cladding layer and Si substrate:

A p-n junction property is clearly observed.

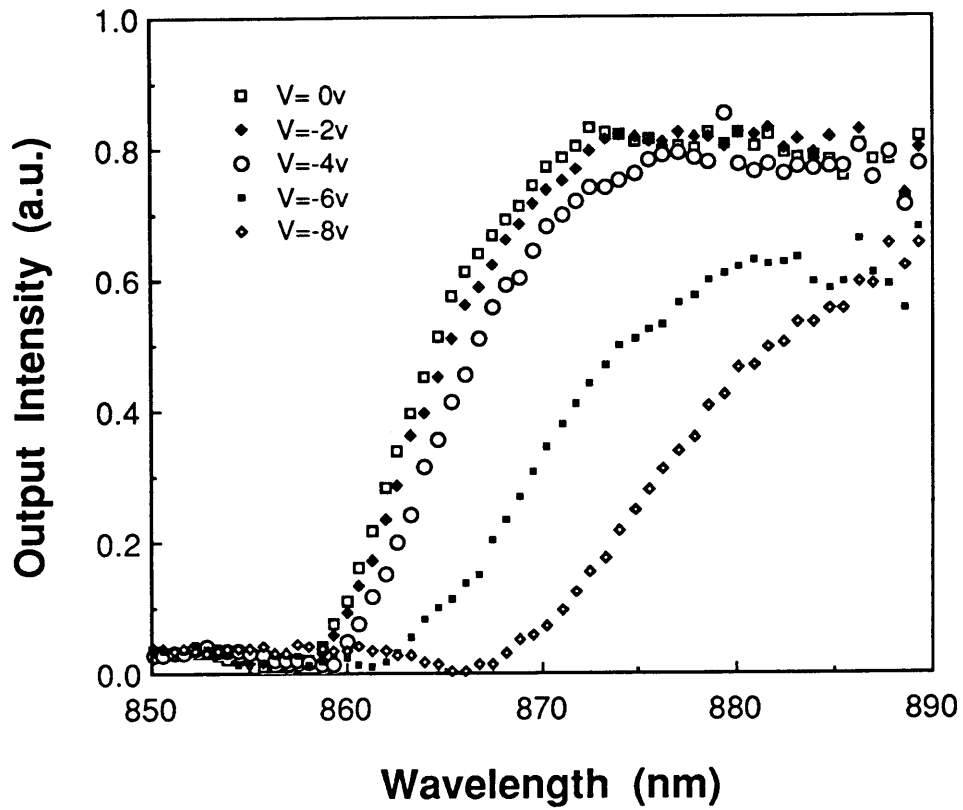
These results show that almost all of the applied reversed voltage affects only p-i-n region.

#### 4-3-2. Application voltage and the light transmission

Fig.4-6 shows the light transmission properties of the waveguide switch as a function of the input light wavelength in various applied voltages. The well width of this sample was 8.3nm. In Fig.4-6, the light absorption begins at the wavelength of 872nm in 0V bias. If compared with the measured value by photocurrent (Fig.3-9), this is just the wavelength where the photocurrent increases. The light transmission intensity at 870nm is more than seven times larger than that of at 860nm in 0V bias.

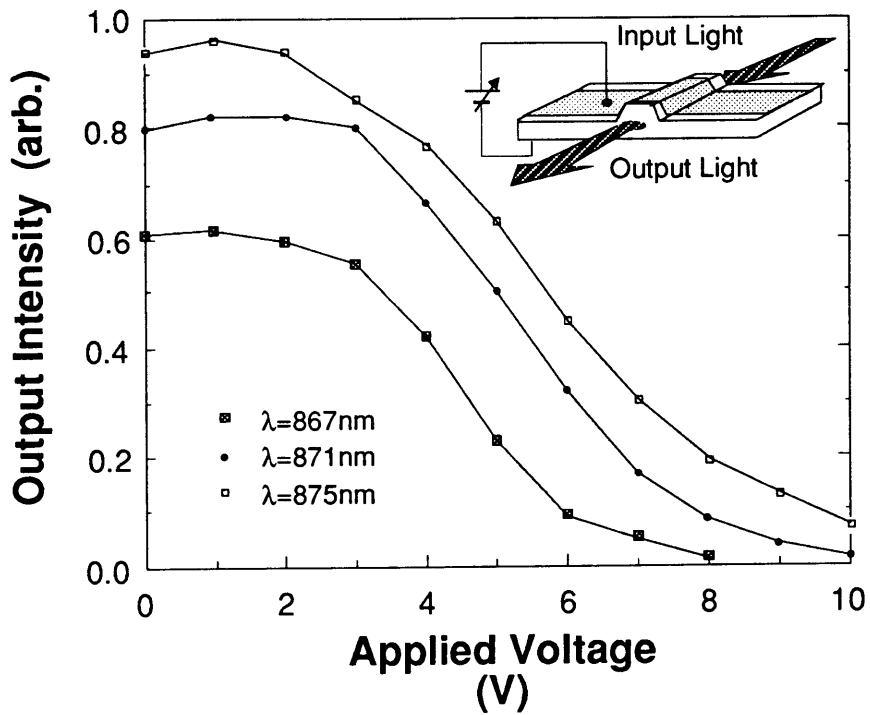
As the applied voltage increases, the absorption edge moves to a longer wavelength. And at the wavelength of 867nm, 33.1dB/mm modulation can be observed at -8V bias to the sample. This result shows that clear switching properties were obtained. Fig.4-7 shows the relation between applied voltage and output intensity at the wavelengths  $\lambda=867\text{nm}$ , 871nm and 875nm. In these wavelengths, the switch shows about 20dB/mm switching modulation within -10V DC bias.

Fig.4-8 and Fig.4-9 shows the same structural switch with a different well width ( $L_w=14.0\text{nm}$ ). The results show



**Fig.4-6. Light transmission property of the waveguide type switch.**

The relation between output intensity and the input light-wavelength in 0V~8V.



**Fig.4-7. Light transmission property of the waveguide type switch.**

Relation between applied voltage and output intensity.

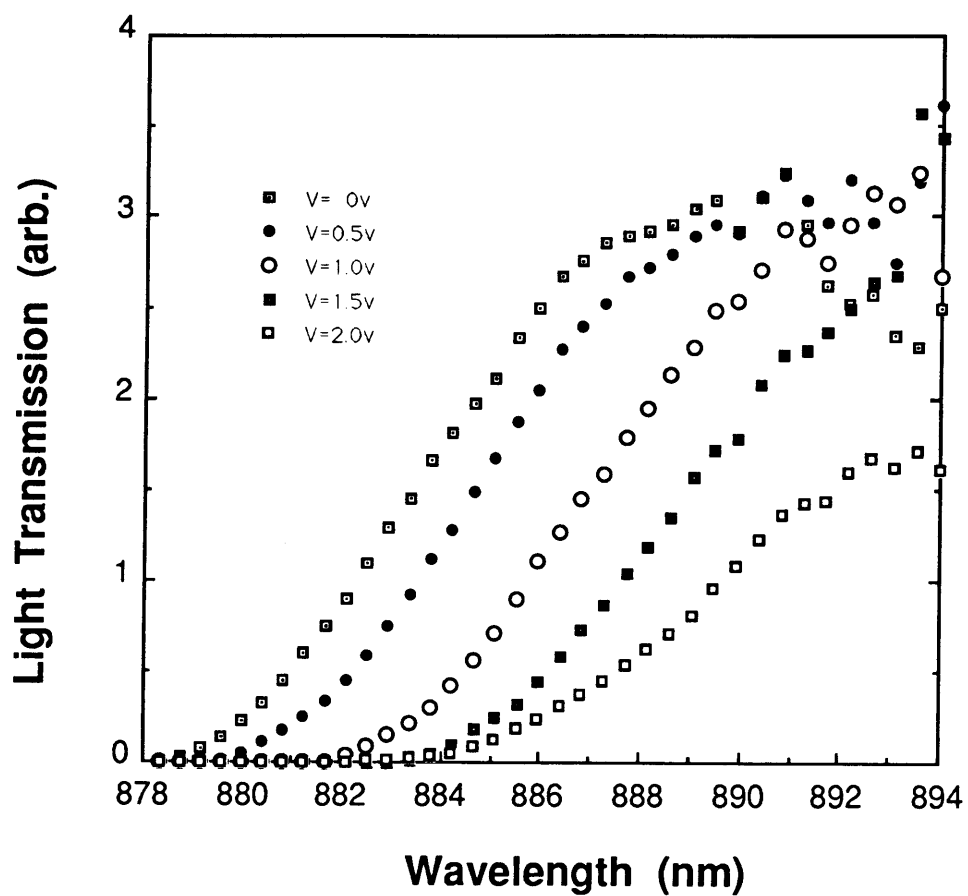


**Fig.4-8. Light transmission properties of the waveguide type switch of  $L_z=14.0\text{nm}$**

The relation between output intensity and the input light wavelength in 0V~2.0V.

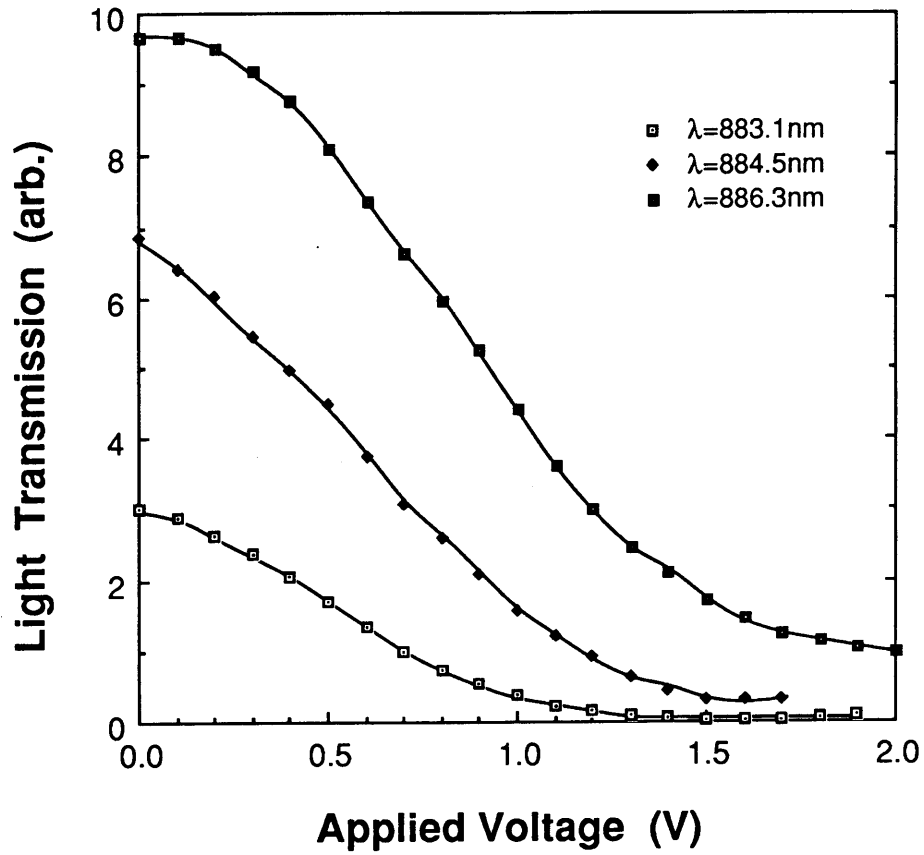


Fig.4-9. The relation between the applied voltage and output intensities in different wavelength. ( $L_z=14.0\text{nm}$ )

clear switching properties on smaller bias applications, since the absorption shift by the QCSE affects strongly a wider well. This switch shows 26.7dB/mm switching modulation within 1.5V bias at 884nm wavelength which is more suitable for practical uses.

Fig.4-10 shows changes of the nearfield patterns of the switch in different well widths ( $L_w=14.0\text{nm}$ ).

#### 4-4.Application to the switch for 850nm wavelength

The propagation losses in the optical fiber are mainly due to Rayleigh scattering loss and the absorption loss. The amount of the losses have minimum points at the wavelengths around  $0.85\mu\text{m}$ ,  $1.05\mu\text{m}$ ,  $1.30\mu\text{m}$  and  $1.55\mu\text{m}$ . In this meaning, these wavelengths are important for optical devices. Among these wavelengths,  $0.85\mu\text{m}$  can be applied for the AlGaAs. If the optical switches on Si are applied to the OEIC's, it is necessary to fit for a 850nm wavelength. The suitable wavelengths for the switches using GaAs QW (which are discussed in 4-3) are 884~889nm for 14.0nm width QW and 862~872nm for 8.3nm width QW. They are not well adapted for the 850nm wavelength.

To make the absorption energy larger for the switch, two methods can be considered. One is to make the width of the QW narrower. In this method, An adequate well width is estimated to be 4.0~5.0nm from Fig.3-1. But as the well width becomes narrower, the shift of the absorption edge due

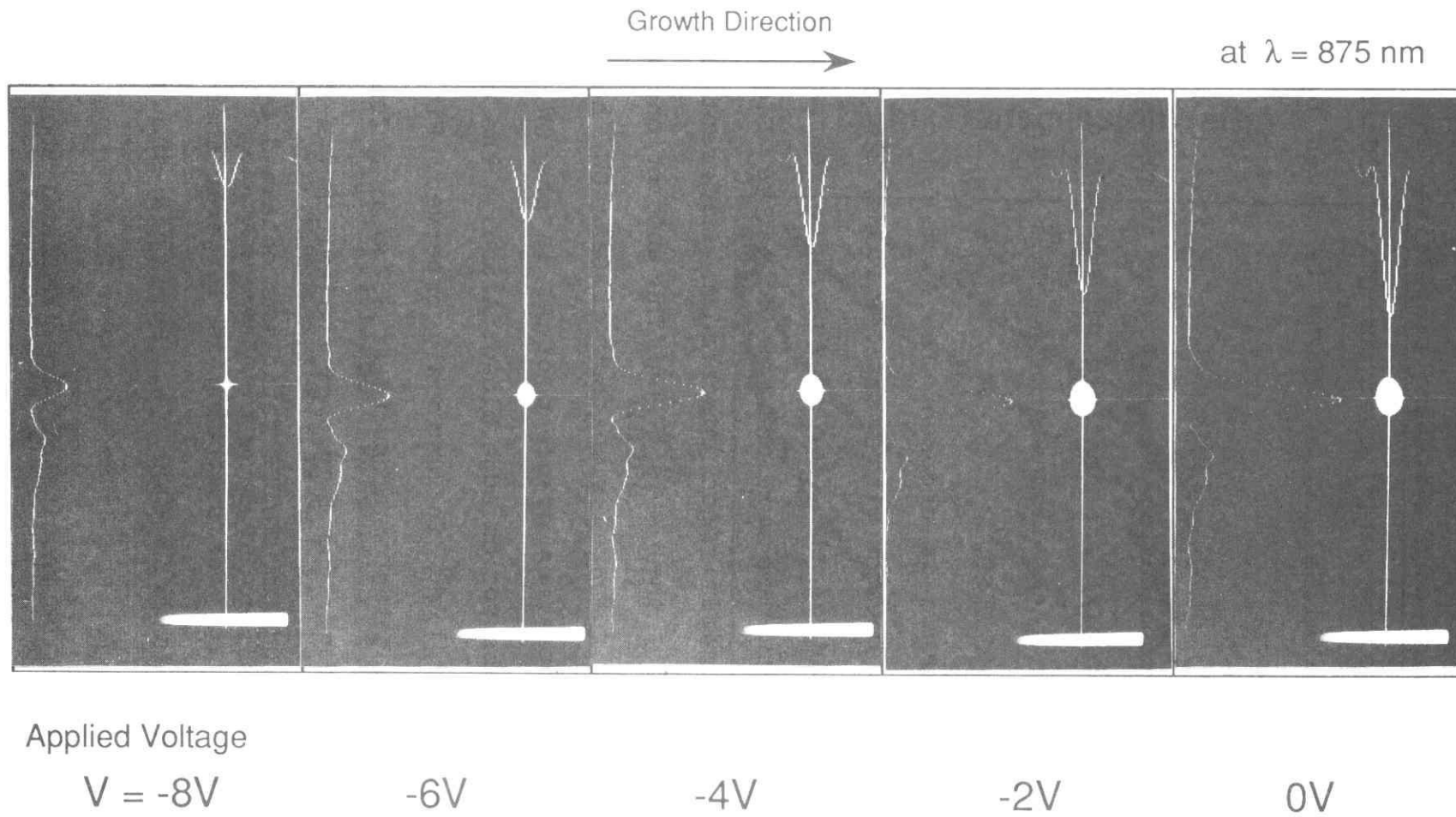


Fig.4-10. The change of the near field pattern and its intensity profile as a function of the applied voltage to the waveguide switch.

to the QCSE becomes smaller. So that the narrower QW cannot be expected as having good switching properties. The other method is to change the material of the QW to AlGaAs. The energy gap of the  $\text{Al}_x\text{Ga}_{1-x}\text{As}$  at  $300^\circ\text{K}$  is given by the following equation:

$$E_g = 1.424 + 1.247x \quad (0 < x < 0.45) \quad 4-1.$$

In addition to this, considering the shift due to the stress, the Aluminum contents ( $x$ ) are confined within 0.03~0.05 for the 850nm switch in the 5~15nm width QW. This width of the QW is expected a good QCSE.

The latter method is chosen. The Aluminum contents were fixed in 0.05, because with a smaller value, it becomes difficult to control the flow of  $\text{AsH}_3$ . The measurement method and sample structure were the same as before. Fig.4-11 shows the light transmission spectra in different bias voltage. The width of the QW is 5.0nm. The absorptions were not so sharp as if compared with that of GaAs QW, because there was a concentration gradient of Al in the QW. This gradient made the absorption edge broad. Although the change of the transmitted light is obviously observed. Fig.4-12 shows the light transmission property at 850nm as a function of the applied voltage. The length of the switch was 0.5mm. In this switch, 29.0dB/mm ON/OFF ratio was obtained by -10V bias. The bias voltage for switching is larger than that of the switch made from GaAs QW. But this shows the satisfactory result for the 850nm switch on Si.

Fig.4-13 shows the results of more practical approaches

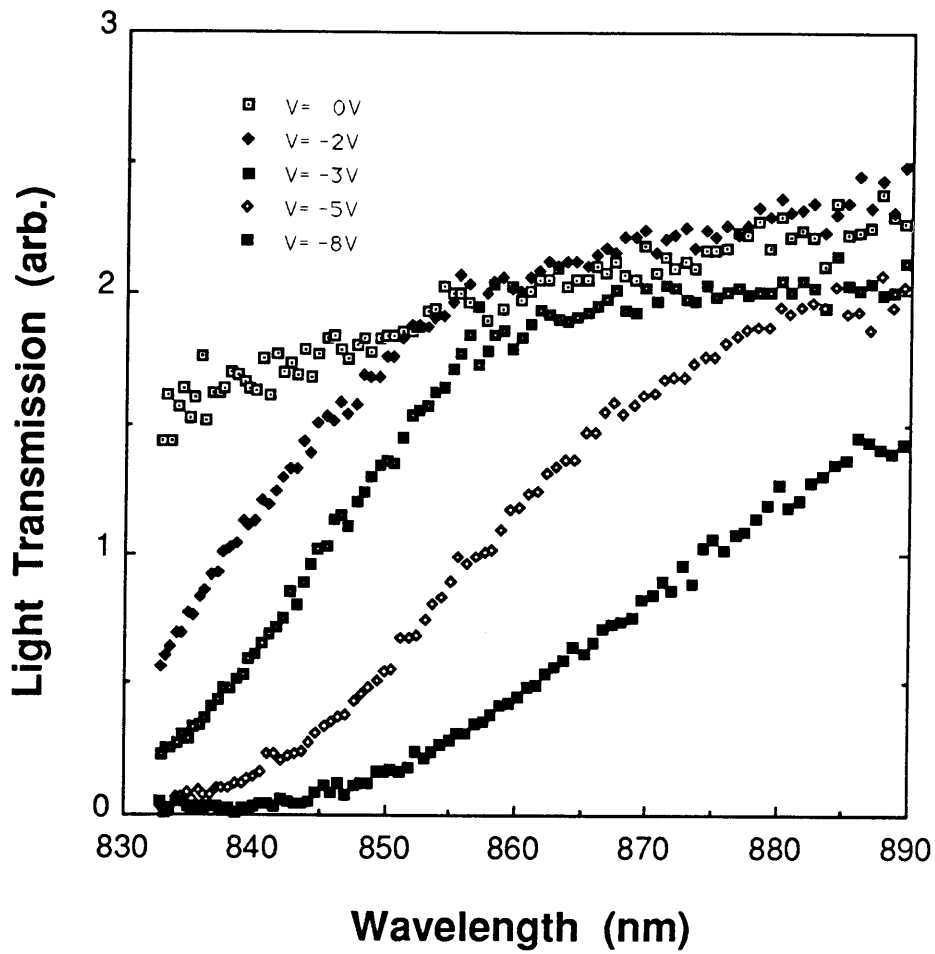


Fig.4-11. Light transmission properties of  $Al_{0.05}Ga_{0.95}As$  SQW ( $L_z=5nm$ ) in the  $Al_{0.25}Ga_{0.75}As/Al_{0.3}Ga_{0.7}As$  DH optical switch.

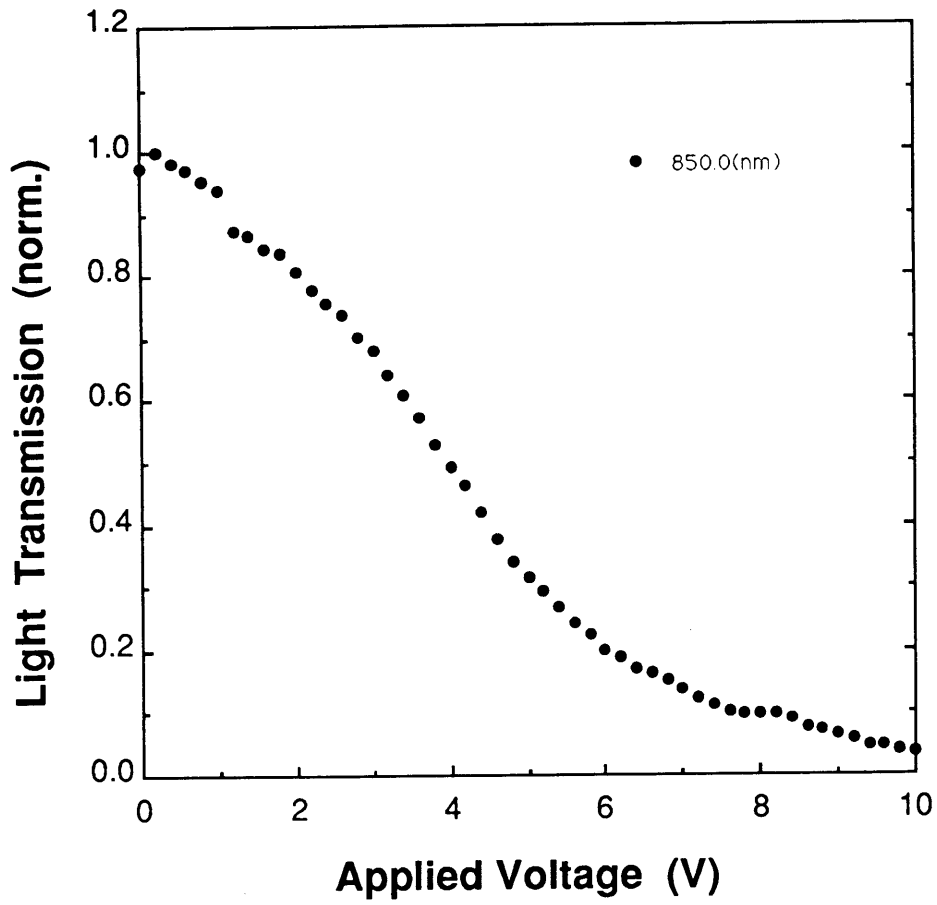


Fig.4-12. Light transmission property at  $\lambda=850\text{nm}$  as a function of the applied voltage.

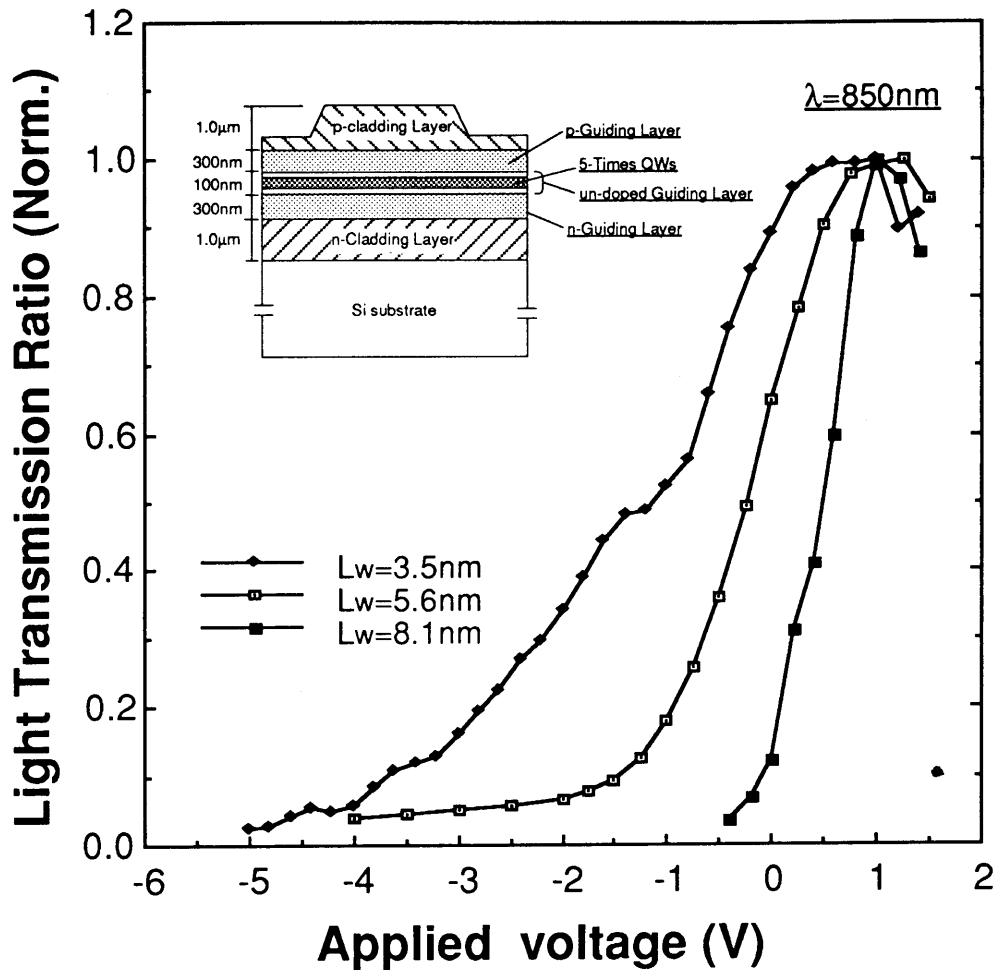


Fig.4-13. The property of the MQW optical switch in different well widths.

MQW consists of five  $\text{Al}_{0.05}\text{Ga}_{0.95}\text{As}/\text{Al}_{0.25}\text{Ga}_{0.75}\text{As}$  structures. The thickness of the undoped region in the guiding layer was 100nm.

for 850nm switch. There are five QWs in 100nm thick undoped layer in the guiding layer. And a 29.3dB/mm switching modulation can be obtained from +1.0V to -0.5V bias at the well width 8.1nm. Due to the built-in potential, the absorption was occurring in 0V bias.

#### 4-5. Integration of InGaAs laser with optical switch

The possibility of integration of a laser diode and an optical waveguide switch, having the same  $\text{In}_{0.05}\text{Ga}_{0.95}\text{As}/\text{Al}_{0.3}\text{Ga}_{0.7}\text{As}$  QW in a double heterostructure, was investigated.

In the case of QW-laser, lasing begins 20-30meV below the  $n=1$  heavy hole excitonic absorptional peak energy under current injection (it is mainly due to the raise of the temperature in the laser.). The absorption peak energy in unexcited condition has a very steep absorption edge due to the step-like densities of states. This means that the QW-laser beam can pass through the waveguide switch in the same structure with no bias, then it is possible to integrate these two components in one chip. The same integration was reported by Tarucha et al. From their report, the achieved modulation was 7dB for a driving voltage of 2.3V and the cut off modulation frequency was 0.88GHz.

One problem is the lifetime of the laser diode on Si substrate. Due to the biaxial stress and high density of dislocations, the lifetime of the laser was very short. Recently, one hopeful report for the lifetime of the laser

was introduced. It was reported that a thin InGaAs layer can release the stress of GaAs on Si so that using the InGaAs as an intermediate layer and active layer, the life time of the laser becomes longer. So the possibility of the integration in the practical uses becomes larger.

In this session, as a first step of the integration, we measured the lasing wavelength of a  $\text{In}_{0.05}\text{Ga}_{0.95}\text{As}$  QW-laser and the switching wavelength of the optical waveguide type switch, and investigated the possibility of integration. Fig.4-14 shows the schematics of the laser diode. The length of the laser diode was  $300\mu\text{m}$ , and the threshold current  $I_{\text{th}}$  was 50mA. The lasing wavelength in 60mA was 880nm (Fig.4-15). On the other hand, the optical waveguide switch was shown in Fig.4-16. The epitaxial layers were the same as the those of the laser shown in Fig.4-14. A  $2\mu\text{m}$ -width ridge was fabricated by wet chemical etching. The switching mechanism was shown before. If these two elements were integrated, the light emission layer in the laser becomes the switching layer of the switch. The light absorption properties measured by the photocurrent in different bias were shown in Fig.4-17. And the light transmission properties are shown in Fig.4-18. In this figure, the wavelength of the laser emission is indicated by the dashed line. The absorption was not sharp compared with the GaAs QW. It is expected to be due to the same reason observed in the case of AlGaAs QW mentioned in Chapter 4-4. But the large change of the light transmission at 880nm shows that the switch can work on this

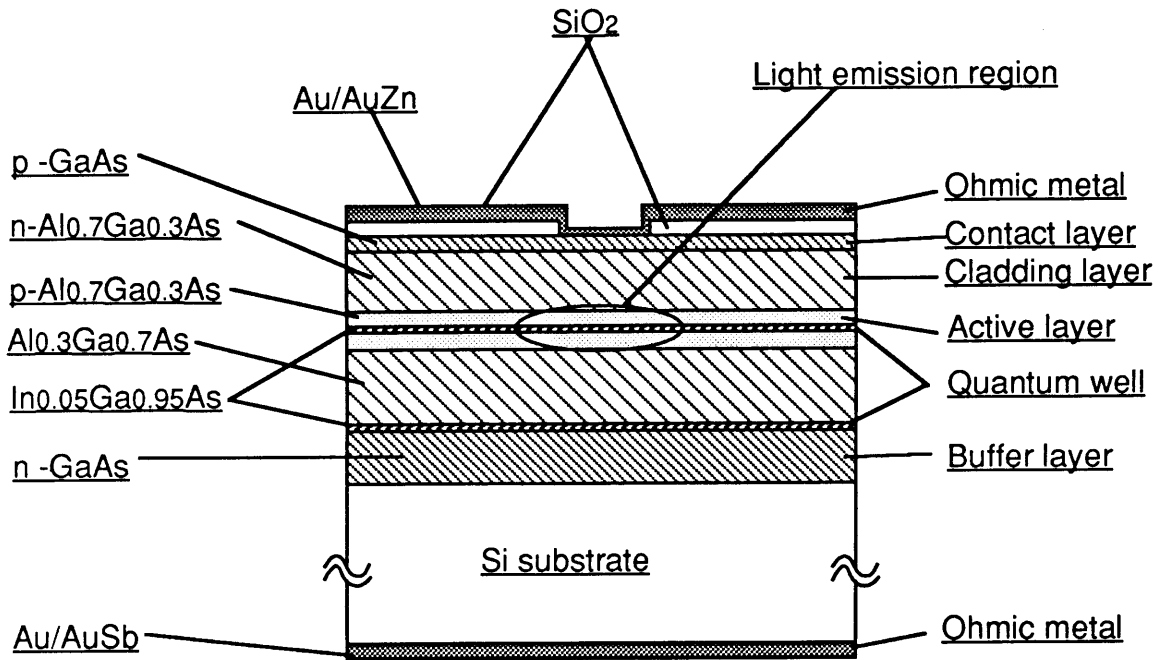
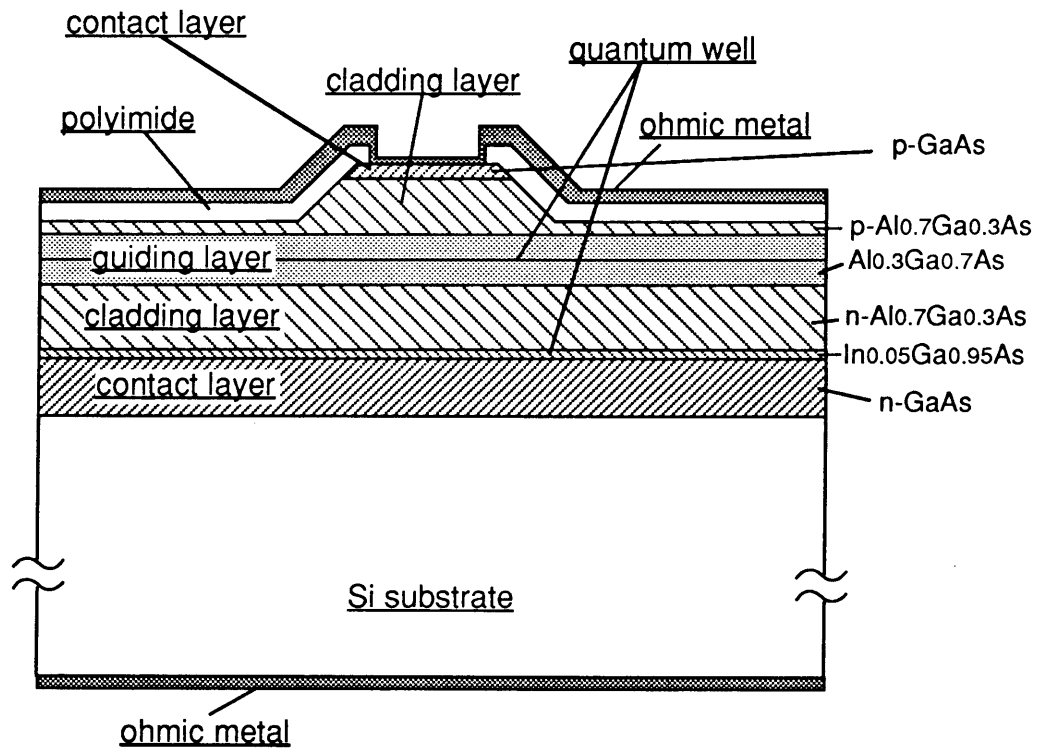


Fig.4-14. The schematic crosssection of the laser diode fabricated on a Si substrate.





**Fig.4-16. The schematic crosssection of the optical switch using In<sub>0.05</sub>Ga<sub>0.95</sub>As QW.**

The vertical structure (growth direction) is the same as that of the laser shown in Fig.4-14.

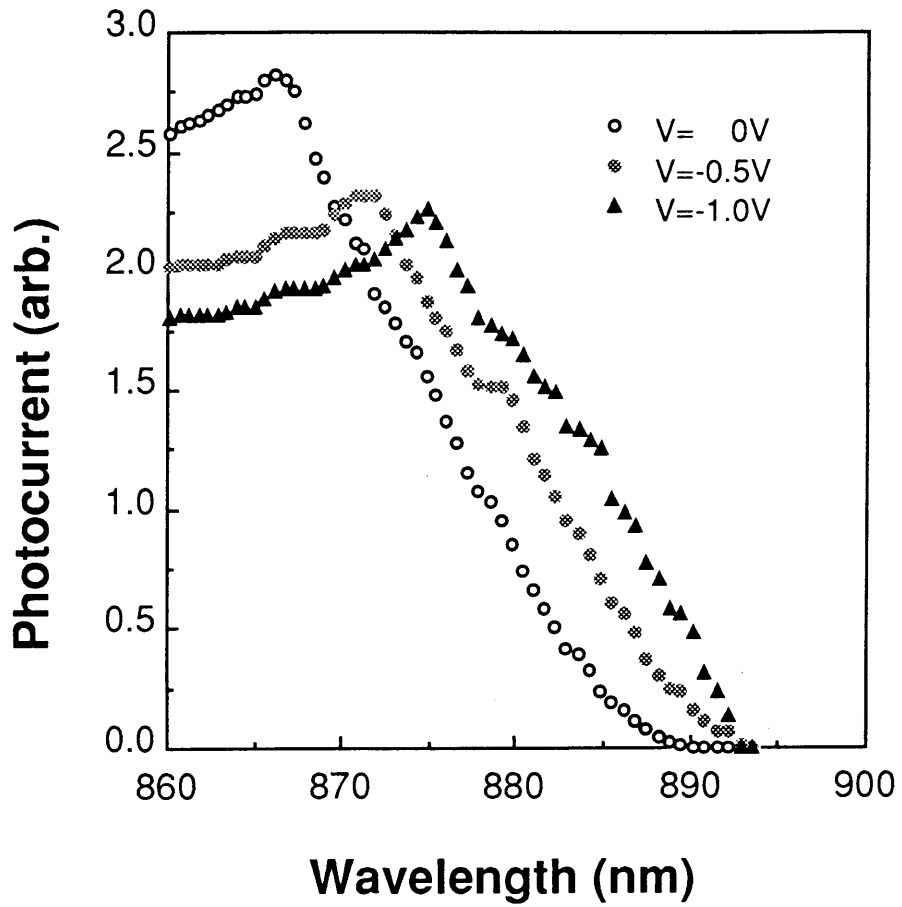
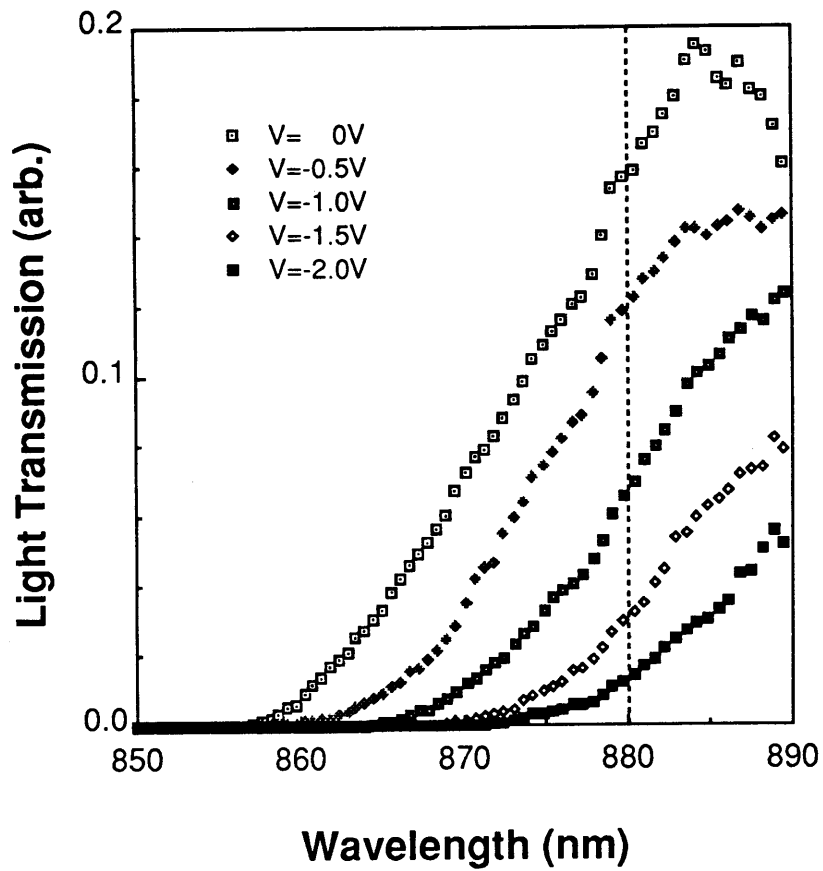


Fig.4-17. The photocurrent spectra versus the wavelength of the input light in various application voltage.



**Fig.4-18.** The light transmission properties of the laser-structure waveguide switch.

The dashed line indicates the wavelength of the laser emission.

wavelength. 21.8dB/mm ON-OFF ratio at 880nm by 2V bias was obtained (Fig.4-19). Those results show that there is a great possibility to the integration.

But there are two problems to connect the laser and the switch. They are:

- 1) As Si substrate has larger thermal conductivity than that of GaAs, the absorption peak of the switch may shift to a longer wavelength.
- 2) The coupling loss may be large, because the way of the traveling light is limited.

The integration process needs more researches to overcome the problems but the result in this session shows the large possibility to make the integration of laser and the switch on Si for the practical uses.

#### 4-6. Conclusion

The application of the optical switch utilizing QCSE on Si substrate was studied.

Waveguide-type 3-dimensional optical switch with 8.3nm and 14.0nm width GaAs/Al<sub>0.25</sub>Ga<sub>0.75</sub>As SQW were shown. The switch exhibited more than 30dB/mm switching modulation with less than -8V bias at  $\lambda=867\text{nm}$  (for  $L_w=8.3\text{nm}$ ), and more than 25dB/mm switching modulation with less than -2V bias at  $\lambda=884\text{nm}$  (for  $L_w=14.0\text{nm}$ ). These results show that the optical switch on Si can apply to the devices in practical use.

Then the application for a 850nm optical switch was

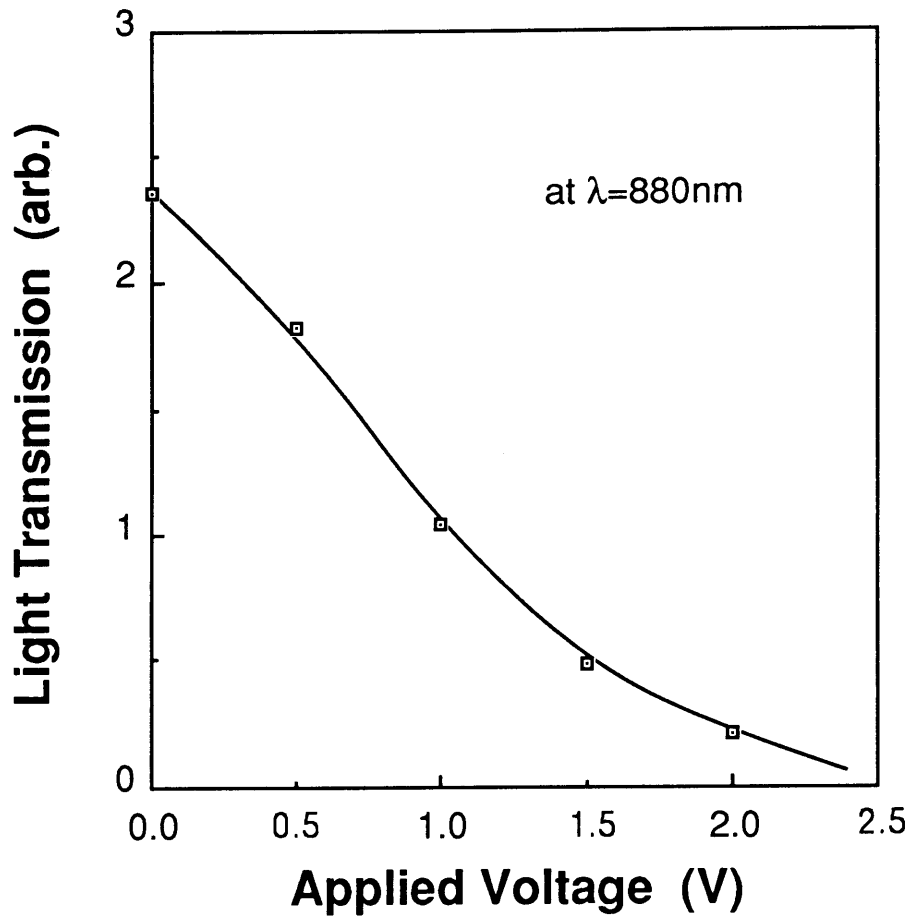


**Fig.4-19. The light transmission properties versus applied voltage at the wavelength of 880nm.**

This wavelength is the same value of the laser emission in the same structure.

attempted. To fit the absorption edge around 850nm, 5.0nm thick Al<sub>0.05</sub>Ga<sub>0.95</sub>As was used for the well. The light absorption of the Al<sub>0.05</sub>Ga<sub>0.95</sub>As QW, which was measured by the photocurrent method, was not as sharp as that of the GaAs QW, but the transmission properties showed a 29.0dB/mm modulation within -10V bias. And more practical approaches were done by using five QWs as the absorption layers and thinner undoped layer to get a stronger electric field by low voltage. This switch showed 29.3dB/mm modulation from +1.0V to -0.5V bias.

And then the properties of the InGaAs QW laser and the optical switch in the same structure were investigated aiming for the future integration. The lasing wavelength of the InGaAs laser was 880nm. While, the absorption edge of the switch in the same structure was 865nm in 0V bias and showed a clear QCSE. As a switch, 21.8dB/mm modulation was obtained at  $\lambda=880\text{nm}$  by -2V bias. This shows the hopeful results for the integration.

In this chapter, some optical switches fabricated on Si were demonstrated. And all of them showed fine properties for switches in practical use.

References.

- 1) T.H.Wood, C.A.Burrus, D.A.B.Miller, D.S.Chemla, A.C. Gossard and W.Wiegmann:Appl.Phys.Lett.,44, (1984),16.
- 2) T.H.Wood, C.A.Burrus, D.A.B.Miller, D.S.Chemla, A.C. Gossard and W.Wiegmann:IEEE.J.Quantum Electron.OE-21, (1985),117.
- 3) S.Tarucha, H.Inamura, T.Saku and H.Okamoto:Jpn.J.Appl. Phys.,24, (1985)L442.
- 4) S.Tarucha and H.Okamoto:Appl.Phys.Lett.,48, (1986),1.
- 5) T.H.Wood, C.A.Burrus, R.S.Turker, J.S.Weiner, D.A.B. Miller, D.S.Chemla, T.C.Damen, A.C.Gossard and W. Wiegmann:Electron.Lett.,21, (1985),693.
- 6) A.Ajisawa, M.Fujisawa, J.Shimizu, M.Sugimoto, M.Uchida and Y.Ohta:Electron.Lett.,23, (1987),1121.

## Chapter.5.Application to the phase modulator

### 5-1.Introduction

There are several different types of electro-optic modulators that can be fabricated in a waveguide structure. The relatively simple waveguide can function as a phase modulator, an amplitude modulator or a switch. So they can be easily connected with each other. One of them, the optical phase modulator, which is a fundamental modulator and is also applicable to other modulators, is an interesting application of GaAs on Si.

In this chapter, we reported the properties of the optical phase modulator of GaAs on Si. The report about the phase modulator of GaAs on Si was one<sup>1)</sup> and which reported that the modulator showed about three times larger shift than the reported value on GaAs substrate<sup>2)</sup>. This reason could not be made clear. But to make sure the effect, and to demonstrate the DH-type phase modulator on Si substrate have great attractions for OEIC's. We prepared a waveguide-type DH optical phase modulator with low carrier concentration, and measured its properties. The phase shift was demonstrated by the change of the refractive index ( $\Delta n$ ) in electric field. And especially, we paid attention to the modulation utilizing the electro-optic effect.

### 5-2. Refractive index

When a voltage  $V$  is applied with reverse bias polarity to the Schottky barrier diode, as shown in Fig.5-1, the waveguide becomes part of the depletion layer of the diode. And the decrease of the carrier density and the application of an electric field cause a change in the phase of light wave traveling along the guide. The change of the refractive index ( $\Delta n$ ) by the voltage application is shown in Eq.5-1.

$$\Delta n = \Delta n_{EO} + \Delta n_{CCR} + \Delta n_{ETC} \quad 5-1.$$

Where  $\Delta n_{EO}$  is the index change caused by the electro-optic effect. And  $\Delta n_{CCR}$  is the change resulting from decreased carrier concentration in the guide and  $\Delta n_{ETC}$  from other effects like Franz-Keldysh effect, for example. When the carrier concentration in 0V bias is large (more than  $1 \times 10^{17}$ ) in the guiding layer,  $\Delta n$  is dominated by the effect of  $\Delta n_{CCR}$ <sup>3)</sup>. But in the low carrier concentration, the effect from  $\Delta n_{CCR}$  is small and then the effect of  $\Delta n_{EO}$  and  $\Delta n_{ETC}$  dominates  $\Delta n$ .

If we neglect the nonlinear terms, the effect of  $\Delta n_{EO}$  is proportional to the applied voltage  $V$ . The change caused by the field in the refractive index for a TE wave (polarized along the  $y$  axis) is given as follow:

$$\Delta n_{EO} = n^3 r_{41} E / 2 \quad 5-2.$$

While there is no change in  $\Delta n_{EO}$  for TM wave (polarized in

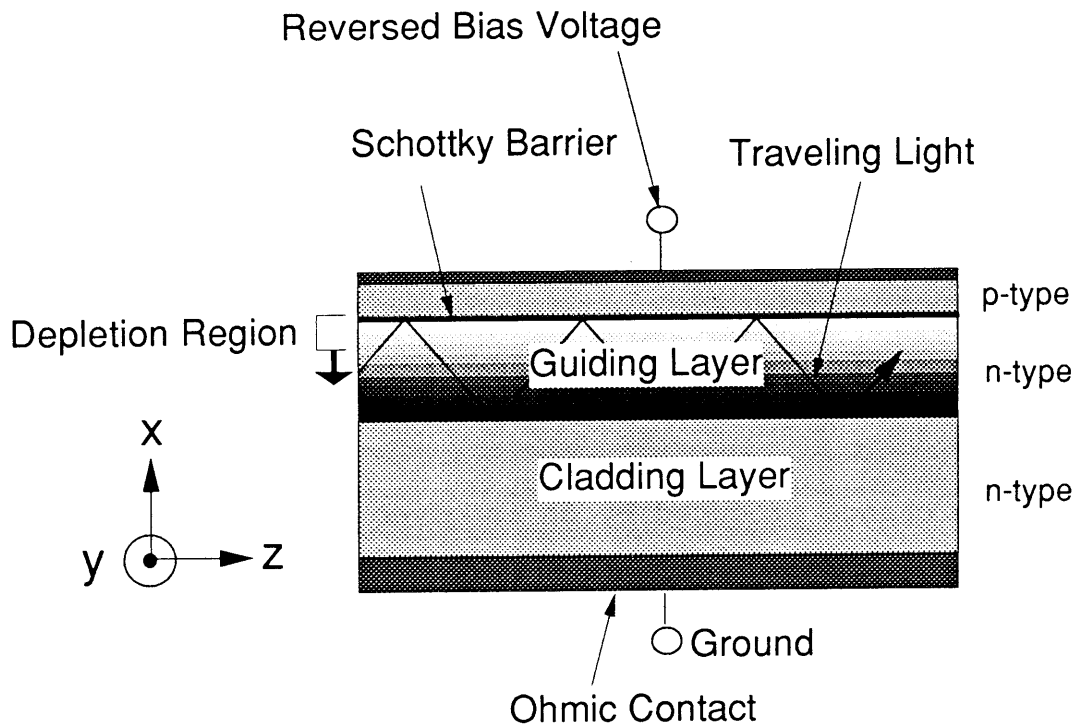


**Fig.5-1. The schematics of basic electro-optic modulator structure.**

As the application of the reversed bias increases, the depletion region occupies the larger part of the guiding layer.

the x direction). In this equation,

$n$  : the refractive index in the guiding layer

$r_{41}$ : electro-optic constant

$E$  : the electric field in the guiding layer

The change of the refractive index is:

$$\Delta n = \Delta\beta/k = (\Delta\beta\lambda_0)/2\pi \quad 5-3.$$

The phase change produced by  $\Delta n$  is given by

$$\begin{aligned} \Delta\phi &= \Delta\beta L = (\Delta n_{EO} + \Delta n_{CCR} + \Delta n_{ETC}) \times 2\pi L/\lambda_0 \\ &= \pi n^3 r_{41} E L/\lambda_0 + 2\pi \Delta n_{CCR} L/\lambda_0 + 2\pi \Delta n_{ETC} L/\lambda_0 \\ &= \Delta\phi_{EO} + \Delta\phi_{CCR} + \Delta\phi_{ETC} \end{aligned} \quad 5-4.$$

Where  $\beta$  is the propagation constant,  $L$  is the length of the modulator in the Z direction and  $\Delta\phi$  is the phase shift. To make an optical modulator, the effect from  $\Delta\phi_{EO}$  becomes very important. That is because the modulating time by the  $\Delta\phi_{EO}$  is pretty shorter than that by others.

### 5-3. Sample preparation and measurement

The sample structure is shown in Fig.5-2. The basic

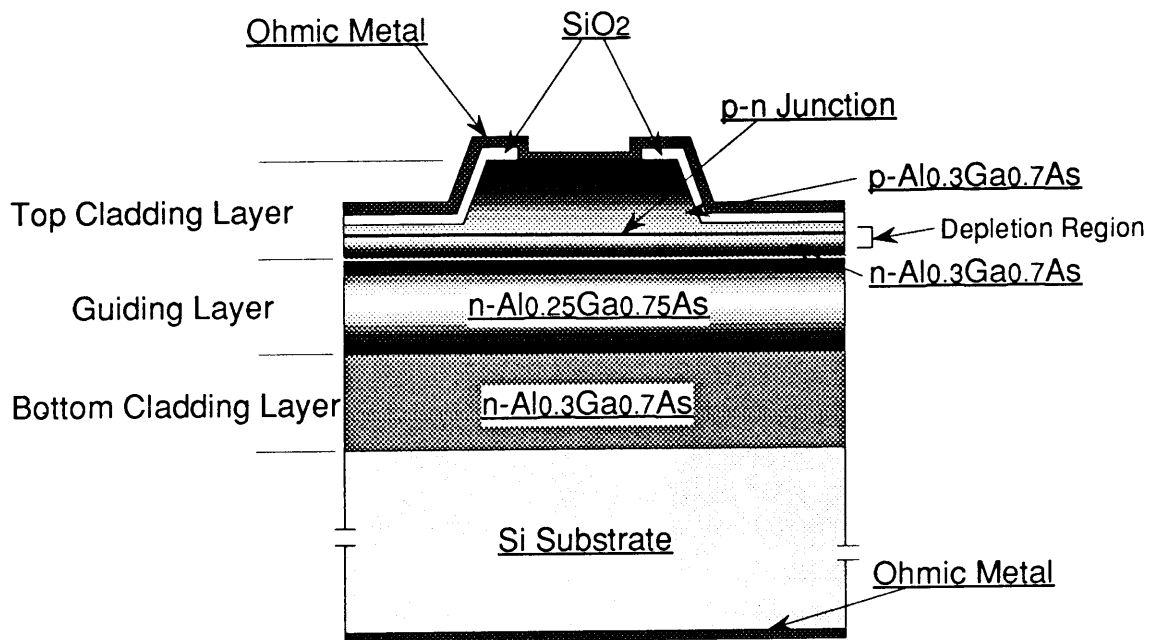


Fig.5-2. The schematical crosssection of the prepared optical phase modulator.

Table .5-1. The conditions of the every layers.

	Thickness	Conduction type	Carrier concentration
Top cladding layer	: 1.0 $\mu\text{m}$ :	p	: $2 \times 10^{17}$
	: 0.03 $\mu\text{m}$ :	n	: $2 \times 10^{16}$
Guiding layer	: 0.7 $\mu\text{m}$ :	n	: $2 \times 10^{16}$
Bottom cladding layer	: 1.0 $\mu\text{m}$ :	n	: $2 \times 10^{17}$

structure is a DH waveguide type optical modulator. The carrier concentration of every layer was shown in table.5-1. All the layers were grown by MOCVD. The thickness of top cladding layer, guiding layer and bottom cladding layer were 1.0 $\mu$ m, 0.7 $\mu$ m and 1.0 $\mu$ m, respectively. A 5 $\mu$ m ridge was fabricated by chemical wet etching. And SiO<sub>2</sub> and ohmic metal were fabricated on the sample. In this structure, the traveling light was confined to a fundamental mode in the vertical (growth) direction under the ridged region. The sidelong view picture of SEM is shown in Fig.5-3.

A p-n junction was fabricated in the top cladding layer. Top electrode-side was p-type and guiding layer-side was n-type. When reversed bias V is applied, the guiding layer becomes a part of the depletion layer. The length of the depletion layer is easily calculated. In the depletion layer, there are no carriers. The refractive index of the guiding layer was affected by  $\Delta n_{EO}$ ,  $\Delta n_{CCR}$  and  $\Delta n_{ETC}$ . A schematic setup for measurement is shown in Fig.5-4. The phase shift was evaluated by measuring the interference fringe at 850nm wavelength. The interference fringe patterns were monitored on a TV by an infrared vidicon and their intensity profiles were recorded by a computer through an image analyzer.

#### 5-4. Results.

The observed interference fringe patterns with and

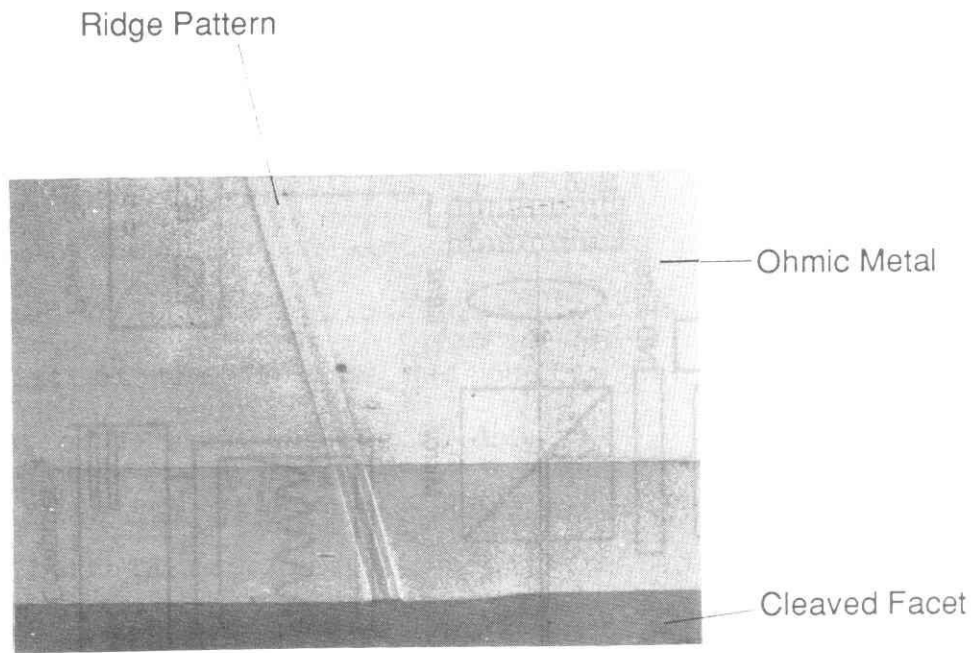


Fig.5-3. The side-long view SEM picture of the optical modulator.

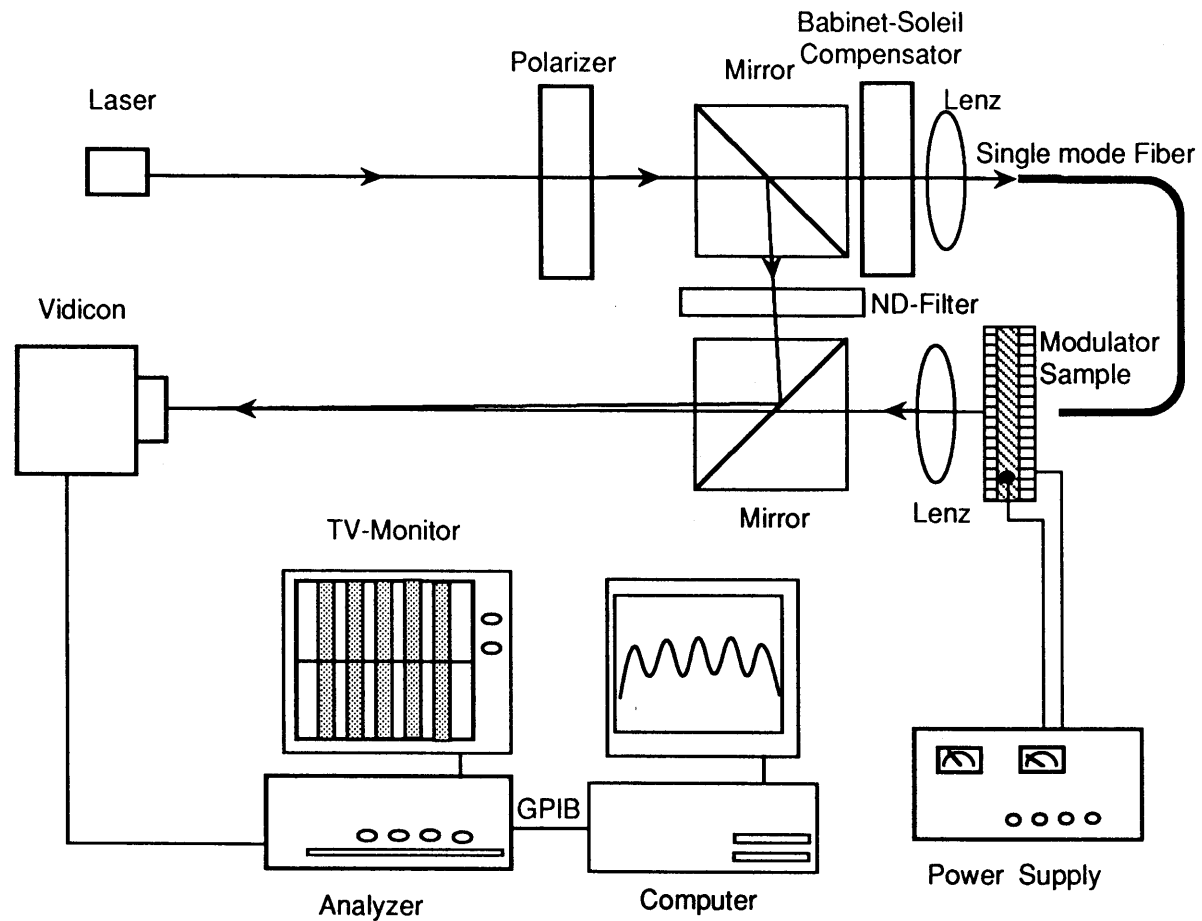


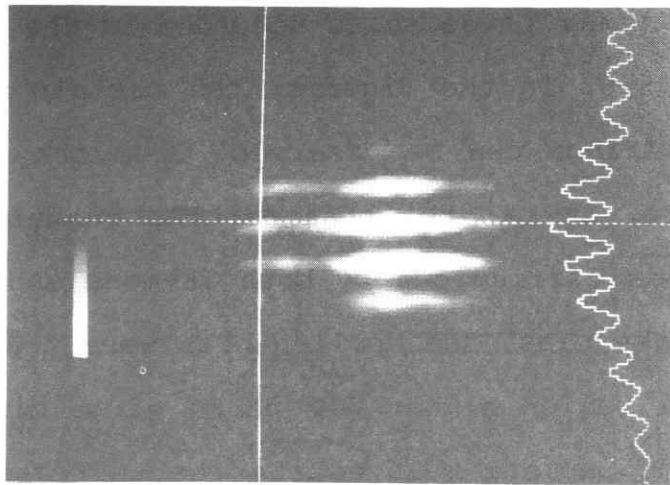
Fig.5-4.Schematic setup for measurement of the phase shift.

without reversed bias are shown in Fig.5-5 a) and b), respectively. And their phase shift recorded in the computer are shown in Fig.5-6. In the figures, the certain shift of the interference fringe can be observed. From the shift of the fringe pattern,  $\Delta\phi$  can be obtained. The measurement of the phase shift was carried out by both TE-mode and TM-mode in different reverse bias. The applied bias were from -6V to -9V, and in these region almost all parts of guiding layer was covered by the depletion layer. So the increase of the phase shift of the TE mode was due to the  $\Delta n_{EO}$  and  $\Delta n_{ETC}$ , while that of TM mode was due to  $\Delta n_{ETC}$ .

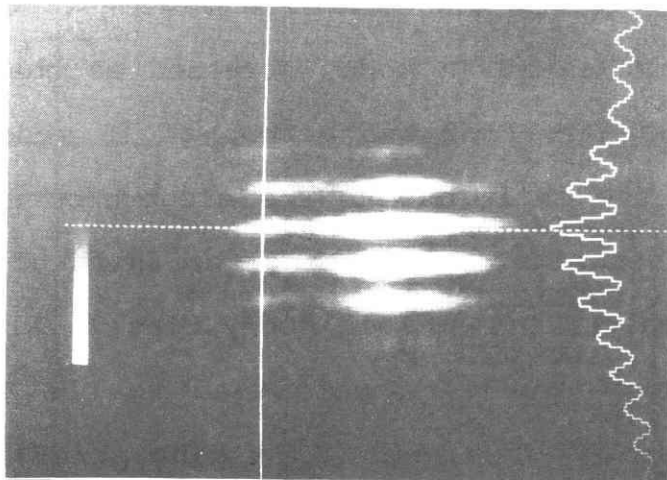
The obtained values are shown in Fig.5-7. The phase shift of both TE mode and TM mode increased as the applied voltage becomes larger. From two graphs of TE mode and TM mode, we can get the shift due to the electro-optic effect  $\Delta\phi_{EO}$ , which is given after subtracting the shift of TM from that of TE. The calculated  $\Delta\phi_{EO}$  in every bias is also shown in Fig.5-7. As the  $\Delta\phi_{EO}$  is proportional to the electric field,  $r_{41}$  is easily obtained ( $r_{41} \propto d(\Delta\phi_{EO})/dE$ ), and E depends on the applied voltage and depletion length  $L_d$  which depends on the carrier density of the top cladding layer and the guiding layer. The calculated  $\Delta n$ ,  $\Delta n_{EO}$  and  $r_{41}$  at -8V bias were  $5.07 \times 10^{-4}$ ,  $2.18 \times 10^{-4}$  and  $1.08 \times 10^{-12}$ , respectively.

#### 5-5. Conclusion.

We have fabricated the optical phase modulator of



a)



b)

**Fig.5-5. The observed interference fringe pattern.**

a).Zero bias application, b).8V reversed bias application. Phase shift can be recognized.

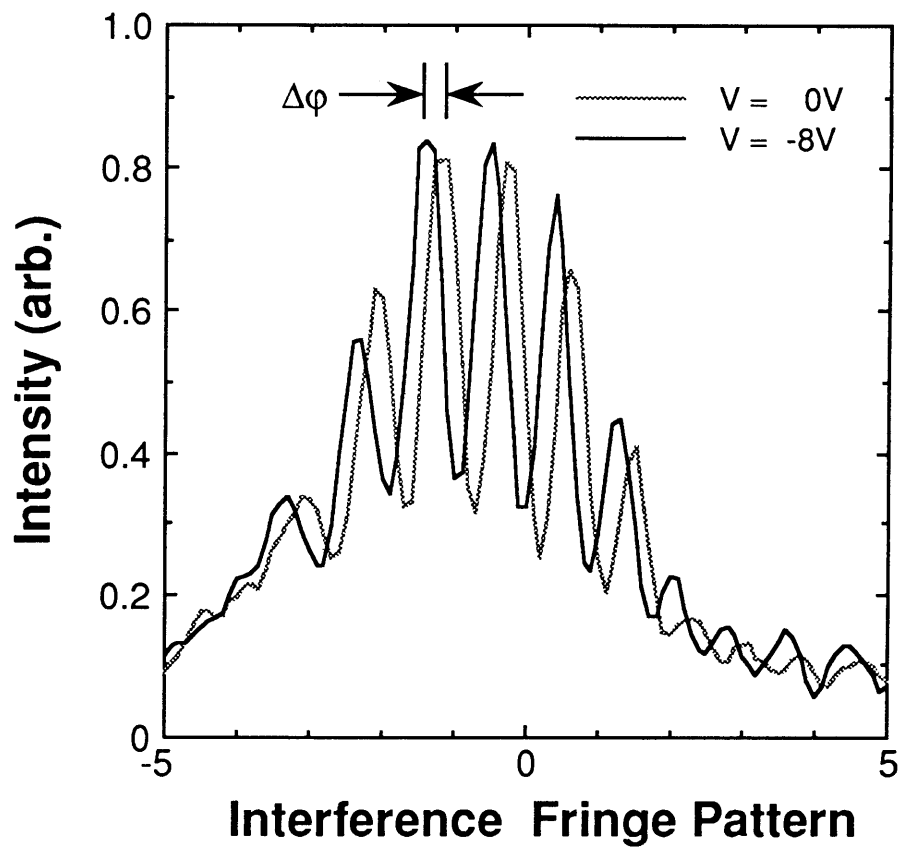


**Fig.5-6. The observed interference fringe with and without reversed bias.**

The phase shift is measured by this fringe.

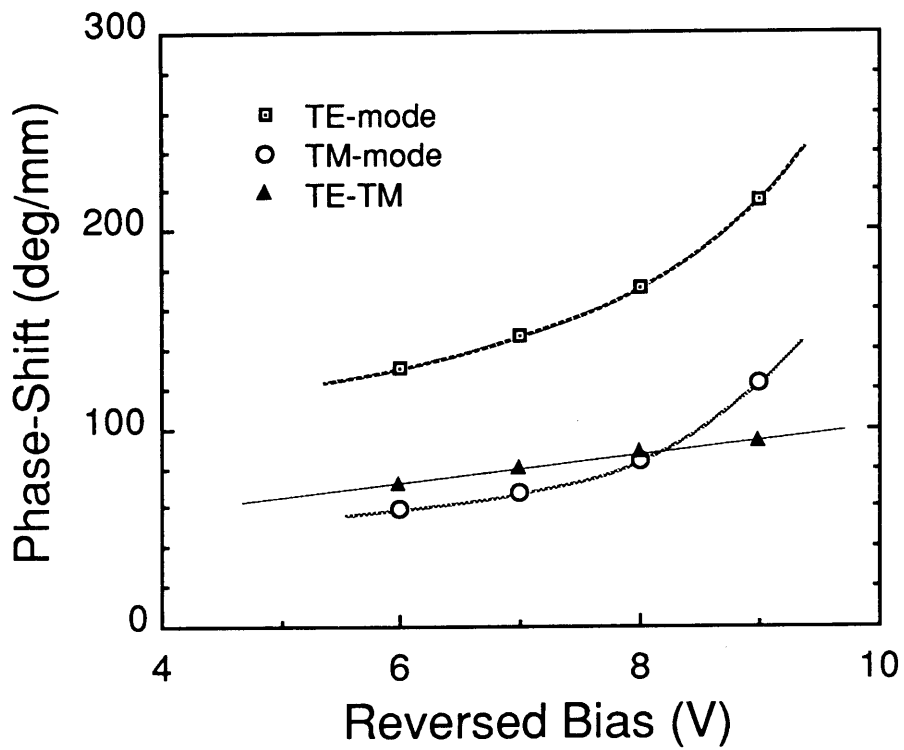


**Fig.5-7. The phase shift of the fringe pattern of both TE-mode and TM-mode.**

The difference between the TE's phase shift and TM's one are due to the Pockels effect.

Al<sub>0.3</sub>Ga<sub>0.7</sub>As/Al<sub>0.25</sub>Ga<sub>0.75</sub>As DH structure on Si substrate. This modulator showed about 200° degree/mm phase shift by 8V bias application. The change of the refractive index ( $\Delta n$ ) was  $5.07 \times 10^{-4}$ . And in this value, the electro-optic effect occupied about 90° degree/mm.  $\Delta n_{EO}$  was  $1.68 \times 10^{-4}$ , and from this value, the  $r_{41}$  was found to be  $1.08 \times 10^{-12}$ . This is not an extraordinary value but it is almost the same as the bulk one. So such a kind of phase modulator was proved to function like the one fabricated on GaAs substrate. But the application to devices in practical use needs more improvement, because the  $\Delta n_{EO}$  is small if compared with that of the dielectric materials like LiNbO<sub>3</sub> etc.

One of the important results was that the optical phase modulator on Si substrate can work almost the same as that of on GaAs one by electro-optic effect. Recently, the research about the MQW optical phase modulators has become popular, because it was reported that the refractive index near the absorption edge shows large change by the electric field application<sup>4)~7)</sup>. The obtained results in this chapter show the great potential for such application.

## References

- 1) Y.S.Kim, S.S.Lee, R.V.Ramaswamy, S.Sakai, Y.C.Kao and H. Shichijo:Appl.Phys.Lett.,50, (1991), 802.
- 2) S.Y.Wang, S.H.Lin and Y.M.Haung:Appl.Phys.Lett.,51(1987), 83.
- 3) D.D.Sell, H.C.Casey, Jr. and K.W.Weicht:J.Appl.Phys.,45, (1974), 2650.
- 4) H.Yamamoto, M.Asada Y.Suematsu:Electron. Lett.,21, (1985), 579.
- 5) H.Nagai, M.Yamanishi, Y.Kan, and I.Suemune:Electron. Lett.,22, (1986), 888.
- 6) T.Hiroshima:Appl.Phys.Lett.,50, (1987), 968.
- 7) J.E.Zucker, T.L.Hendrickson, C.A.Burrus:Appl.Phys.Lett., 52, (1988), 945.

## Chapter 6. Summary

The studies of GaAs on Si has continued for more than ten years since 1982. In this period, many remarkable works have been reported. They are about the crystal growth and device applications. Especially, at the beginning of this research work, numerous important and fundamental techniques to grow the GaAs on Si were introduced. Among them, two-step method, thermal cycle annealings and strained layer supper lattice (SLS) are indispensable to get the high quality GaAs. But in the last few years, the reported works about GaAs on Si have gradually decreased. This is because the two difficult problems (that are the stress and dislocations) have not been settled yet and whose prospect is not so good. To continue this work, we have to settle those problems. Or we have to think from a different point of view for the device application. In this meaning, waveguide type devices (which are not affected by such difficultes) have much attraction.

In this thesis, the device application of GaAs on Si, which need little power and are not affected by the dislocations and stress, aiming to make the OEIC's were studied. The properties of DH optical waveguide, that is one of the most fundamental devices for the optical interconnections, was investigated for the first time. And waveguide type optical switches or optical phase modulators were fabricated on Si substrate. All of them were made by

MOCVD.

In chapter.1, the reported results up to the present about the GaAs on Si and the purpose of this thesis were described. The important results obtained by the experiments are summarized as follow:

In chapter.2, the characteristics of GaAs on Si DH type optical waveguide were studied. The near field patterns and their intensity profiles at  $\lambda=1.3\mu\text{m}$  were investigated. The obtained profiles agreed quite well with these of the calculated ones by the effective index method. In the near field pattern, some dark spots were found in the slab type waveguide. They were 2~7 $\mu\text{m}$  intervals and were almost the same as the intervals of the surface macrosteps. But in the ridged waveguide, the effect of the dark spots did not affect strongly. Then the propagation losses of the ridged waveguide were measured and they were found to be around 20~25dB/cm. This value is a little larger than the expected ones. The scattering from the surface or ridge wall might be larger. We expect the loss become smaller as the crystal growth technology advances.

In chapter.3, the characteristics of QW of GaAs/AlGaAs on Si were studied. The TEM pictures and PL spectra of the MQW were investigated. In the TEM pictures, there were some windings and splittings that originated from the dislocations. And by PL spectra, the fluctuation in well size in MQW was estimated to be within  $\pm 2a$ . Then the absorption of (GaAs/Al<sub>0.25</sub>Ga<sub>0.75</sub>As) QW ( $L_z=8.3\text{nm}$ ) on Si and

on GaAs in the same structure were measured by the photocurrent method in the room temperature. And they were compared with the calculated absorption wavelength obtained under consideration of the 2.3Kbar stress (that is the same situation of GaAs on Si). About 13.5nm difference of the absorption edge was observed. And the absorptions in different well widths on Si were also compared. They agreed well with the calculated values. These results show that the QW device of GaAs on Si can be easily designed by considering the effects of the stress. And the QCSE of the QW on Si substrate was measured. The p-i-n sample with 8.3nm SQW showed a large shift of the absorption edge as the applied voltage increased. The shift of the absorption edge by 8V bias was about 10nm. And the shift was almost the same as the compared sample fabricated on the GaAs substrate.

In chapter.4, The application to the optical switch utilizing QCSE on Si substrate was studied. Waveguide-type 3-dimensional optical switch with 8.3nm and 14.0nm width GaAs/Al<sub>0.25</sub>Ga<sub>0.75</sub>As SQW were demonstrated. The switch showed more than 30dB/mm switching modulation less than -8V bias at  $\lambda=867\text{nm}$  (for  $L_w=8.3\text{nm}$ ), and more than 25dB/mm switching modulation less than -2V bias at  $\lambda=884\text{nm}$  (for  $L_w=14.0\text{nm}$ ). Then the application for 850nm optical switch was attempted. The switch of 5.0nm Al<sub>0.05</sub>Ga<sub>0.95</sub>As SQW showed 29.0dB/mm modulation within -10V bias. The switch consisted of five QWs in thinner undoped layer showed 29.3dB/mm modulation from +1.0V to -0.5V bias. Then the InGaAs QW laser and the

optical switch in the same structure were investigated aiming for the future integration. The lasing wavelength of the InGaAs laser was 880nm. While, the absorption edge of the switch in the same structure was 865nm in 0V bias and showed 21.8dB/mm modulation at  $\lambda=880\text{nm}$  by -2V bias. This showed the hopeful results for the integration of the laser and switch.

In chapter.5, The optical phase modulator of  $\text{Al}_{0.3}\text{Ga}_{0.7}\text{As}/\text{Al}_{0.25}\text{Ga}_{0.75}\text{As}$  DH structure on Si substrate were demonstrated and showed about  $200^\circ$  degree/mm phase shift by 8V bias application. The change of the refractive index ( $\Delta n$ ) was  $5.07 \times 10^{-4}$  including the electro-optic effect of  $\Delta n_{\text{EO}}$  to be  $1.68 \times 10^{-4}$ , and from this value, the  $r_{41}$  was calculated to be  $1.08 \times 10^{-12}$ . This is not a extraordinary value and almost the same with the bulk one. This result shows that the phase modulators on Si substrate function like that fabricated on GaAs substrate.

Scope for the future work

About this work

DH optical waveguide and related devices like optical switch and phase-modulator on Si substrate were studied. All of the investigated devices have stable properties and they showed the almost expected properties. But the obtained propagation loss was large. The loss was generated from the free carrier absorption and scattering from the surface and ridge wall scattering. The latter factor may affect greater

than we expected. In MOCVD, the macrosteps appear at the surface. They may affect to the scattering larger. The researches to make a plane surface by MOCVD will be needed for the waveguide (lower the growth temperature is one of the methods). And at least lower than 2~3dB/cm loss will be required for the integration.

To say about the QW device, its quality is affected by the density of the dislocations in QWs and the fluctuation of the well size ( $\Delta L_z$ ) (this is a problem of the MOCVD machine.). But these effects for optical switch are not so serious. The QW shows the expected properties and their device application will be possible on Si substrate.

#### About GaAs on Si

The largest problems are high density of dislocations and residual stress. They disturb the applications to active devices (such as laser or LED). To overcome these problems many research workers have struggled, but definite solutions have not been found yet, completely. But many new method to avoid them have been proposed and the GaAs on Si technology has steadily progressed. And new device applications like waveguide modulators or FETs etc., which are not affected by those difficulties, will grow.